REPORT No. 432

FORCE MEASUREMENTS ON A 1/40-SCALE MODEL OF THE U. S. AIRSHIP "AKRON"

By Hugh B. Freeman

SUMMARY

This report describes a series of tests made on a 1/40-scale model of the U. S. airship "Akron" ("ZRS-4") for the purpose of determining the drag, lift, and pitching moments of the bare hull and of the hull equipped with two different sets of fins. Measurements were also made of the elevator forces and hinge moments.

The results of the drag measurements are in fair agreement with those of previous tests on smaller models of the "Akron" conducted in the variable-density tunnel of this laboratory. The type of tail surface designated Mark-II, a short wide surface, was found to have more favorable control characteristics than the long narrow type, Mark-I. The results of the measurements of the elevator hinge moments showed that the elevators for both types of fins were overbalanced for a large range of elevator angles, indicating that the area of the balancing vanes, for the Mark-II elevators at least, was excessive.

INTRODUCTION

The subject tests are a part of a program of research undertaken at the request of the Bureau of Aeronautics, Navy Department, on a 1/40-scale model of the U. S. airship *Akron* (*ZRS-4*) with the object of determining: (1) The lift, drag, and moment on the bare hull and on the hull fitted with two different sets of tail surfaces; (2) the elevator forces and hinge moments; and (3) the pressure distribution over the hull and fins. The program was later extended to include (4) the measurement of total head in the boundary layer at 10 stations on the hull. Parts (1) and (2) are the subject of the present report. The results of the pressure distribution are given in reference 1 and those for the boundary-layer tests in reference 2.

Several advantages were offered by the unusually large size of the model available for these tests and of the 20-foot wind tunnel in which the tests were conducted. These were, namely: (1) The Reynolds Number was large for an atmospheric wind tunnel; (2) the control surfaces were large enough to allow the measurement of the elevator forces and hinge moments; (3) the tare drag could be measured directly, hence probably more accurately than usually is possible on smaller models.

The results are compared to those of previous tests conducted in the variable-density tunnel of the National Advisory Committee for Aeronautics. (Reference 3.)

APPARATUS AND TESTS

The model, built in the shops of the Washington Navy Yard, is of hollow wooden construction, having a polygonal cross section with 36 sides over the fore part of the hull that faired into 24 sides near the stern. The surface was given a fine sand finish, then varnished, painted, and finally finished with fine sandpaper, giving a surface which was probably as smooth as that of a well doped fabric surface. The over-all length of the hull measured from the end of the bow cap is 19.62 feet and the maximum diameter 3.32 feet, giving a fineness ratio of 5.9. The details of the method of construction are shown in Figure 1. The principal dimensions of the model are collected in the following table:

DIMENSIONS OF MODEL U. S. S. "AKRON"

[Scale=1/40]

Distance from nose (length)	Radius (circumscribed circle)	
a/L	*Inches*	
0	0	
0.02	4.95	Length, 19.62 feet.
.05	9.98	Volume, 115 cubic feet.
.10	14.20	
.15	16.65	
.20	18.39	Total horizontal tail-surface area (square feet):
.25	19.12	Mark-I 5.074 — Mark-II 4.590
.30	19.61	
.35	19.85	
.40	19.90	Elevators (including balance vanes) square feet:
.45	19.90	1.004 — 0.932
.50	19.80	
.55	19.59	Elevator balance vanes (square feet):
.60	19.12	0.234 — 0.220
.65	18.46	
.70	17.50	Elevator chord length (feet):
.75	16.15	c=0.410 — c=0.369
.80	14.44	
.85	12.29	Location of elevator axis:
.90	9.61	a/L=0.9090 — a/L=0.9059
.95	6.52	Center of buoyancy:
1.00	0	a/L=0.464

Two sets of tail surfaces, designated Mark-I and Mark-II, were provided with the model, the Mark-II type of surface being that used on the full-scale ship. The forms of these are shown in Figure 2. Figure 3 shows the type of balancing vanes with which the

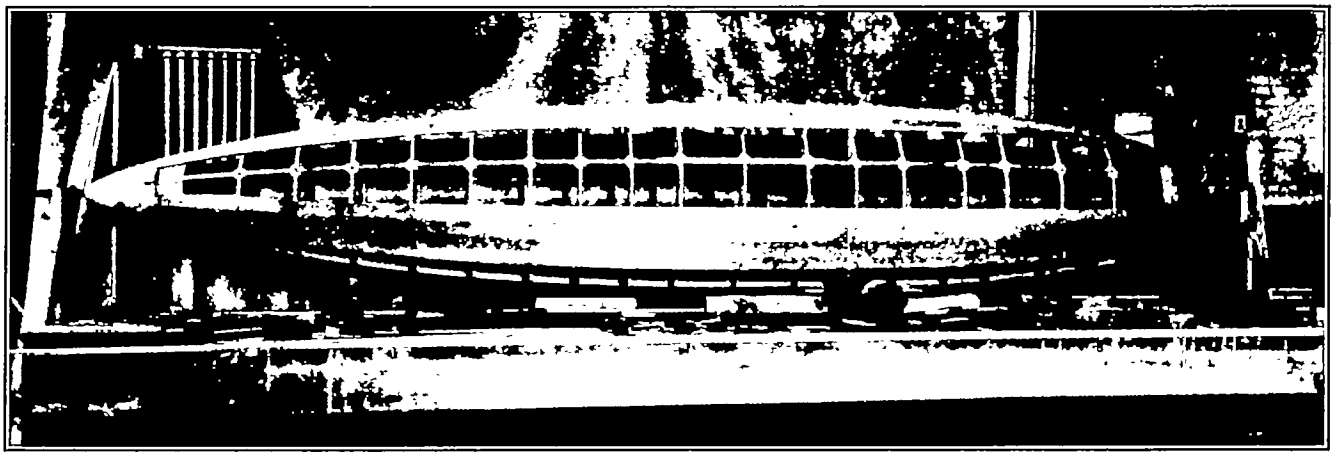

FIGURE 1.—Details of construction of the 1/10-scale model U. S. S. *Akron*

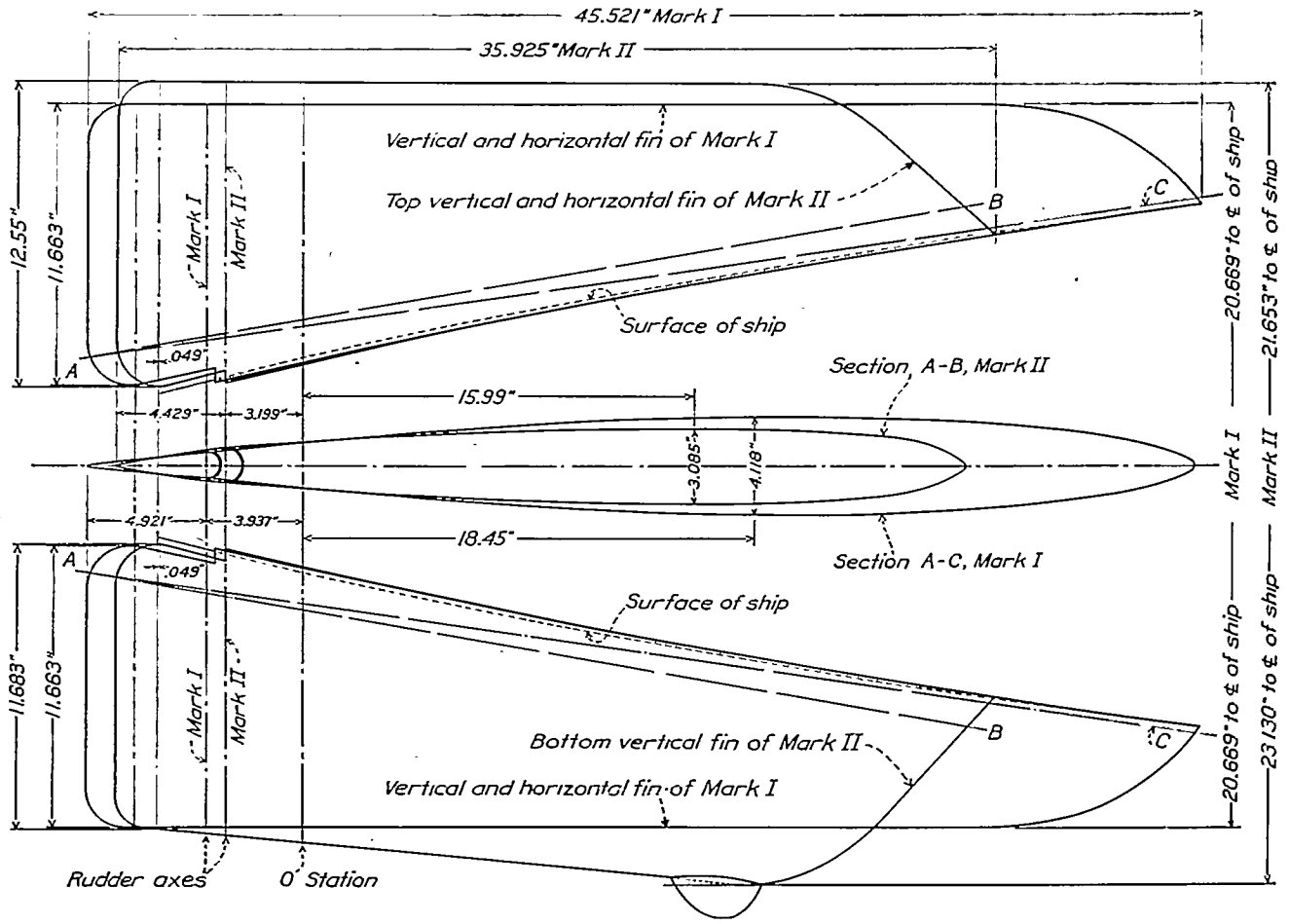

FIGURE 2.—Mark-I and Mark-II fins and control surfaces for the 1/10-scale model U. S. S. *Akron*

elevators and rudders were equipped. The balancing vanes were provided with trailing-edge flaps for the purpose of increasing the effectiveness of these vanes at high angles of the control surfaces. The relation of the flap angle β, which on the full-scale ship is governed by the position of the elevator, to the elevator angle δ is shown by the table in Figure 3.

No propellers or propeller struts were provided with the model, as it was thought that the scale effect on these parts would make the results of questionable utility.

The method of mounting the model in the wind tunnel is shown in Figures 4 and 5. The model was suspended by two vertical wires attached at the upper ends to platform scales on which the left was measured. The front lift wire entered the model through a narrow slot in the upper surface of the hull and was attached to a horizontal steel crossbar, which turned in ball bearings mounted on opposite sides of the hull. The slot in the upper surface was cut in a thin steel plate set into, and flush with, the surface of the model. A second narrow strip of sheet steel sliding on the under surface of the first moved with the wire when the angle of pitch was changed and covered the slot, preventing any flow of air except for a small clearance around the wire which was provided to prevent the friction of the arrangement from interfering with the measurement of the pitching moment.

The ends of the above-mentioned steel crossbar were ground to streamline shapes and extended outside the hull 1¼ inches on each side, affording an anchorage for the two drag wires. These wires were carried forward into the low-velocity region of the entrance cone and transmitted the drag to a bell crank and thence to a balance on the floor of the tunnel. An initial tension was given to the drag wires by the use of a counterweight which was carried by a wire attached to the tail sting and extended down, over a ball-bearing pulley in the exit cone, into the test chamber below. Four cross-tunnel wires held the model rigid laterally. The two side braces at the rear were fixed to a mechanism on the walls of the tunnel, which moved with the hull so as to keep the wires always perpendicular to the axis of the model. A similar device, mounted on the rear lift balance, allowed the wire support at the tail to be kept vertical. The model pivoted on the ball bearings about the crossbar, the angle of pitch being changed by raising or lowering the tail sting.

The elevator forces perpendicular to the axis of the hull and the moments about the elevator hinge axis were measured on a 2-component electric induction balance designed especially for these tests. The general scheme of this apparatus is similar to that described by Relf and Simmons in reference 4. The balance, shown in Figure 6 as assembled for the calibration tests, consists of two parts which, for convenience, have been designated the model unit (shown in the foreground) and the floor unit. The elevator surfaces are shown mounted on the force and torque tube which was supported on two Emery knife-edges, located on the axis and near the ends of the tube. The tube was restrained from turning about its axis by a torque, or moment, arm which may be seen attached,

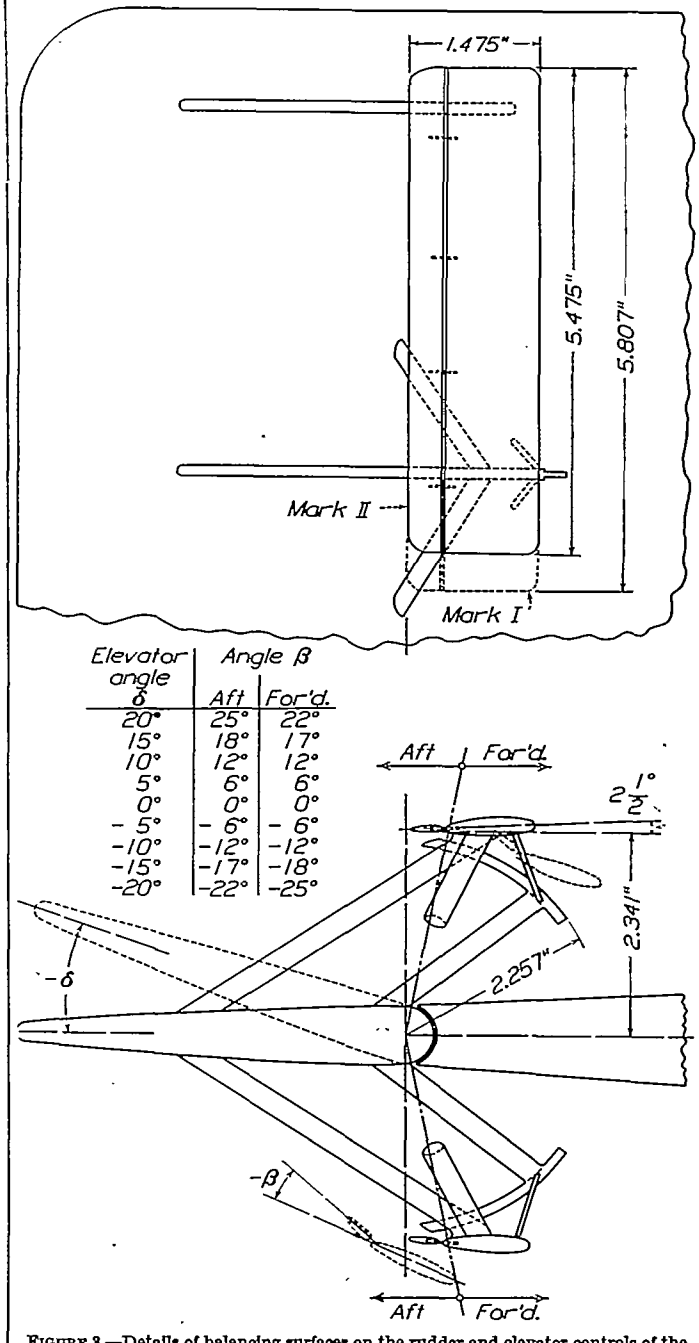

FIGURE 3.—Details of balancing surfaces on the rudder and elevator controls of the 1/40-scale model U. S. S. *Akron*

tangentially, to the center of the tube. The forces and moments were transmitted by this tube to steel spring beams, the deflections of which were measured electrically. The floor unit consisted of two compensating units, two galvanometers (left background), a 110-volt rotary converter to provide the alternating current, and two rectifiers to rectify the current

passing through the galvanometers. The rectifiers consisted simply of a pair of contact points operated by an eccentric attached to the shaft of the converter.

The electrical relation between the various parts of the force component of the balance, which was essentially the same as the moment component, is shown in Figure 7. Four pairs of coils were connected in such a way as to form an induction bridge. Two arms of the bridge were in that part of the balance designated the model unit; the remaining two were in the floor unit. The elevator forces were transmitted to a steel spring, the deflection of which caused the movement of an armature, placed between the coils of adjacent arms of the induction bridge. This movement caused an increase of the inductance in one pair of coils and a decrease in the other. The resulting unbalance, which was indicated by the deflection of a galvanometer, was compensated for by the movement of a similar armature in the floor unit. This movement was measured by means of a micrometer screw. The point of balance of the bridge was indicated by the galvanometer.

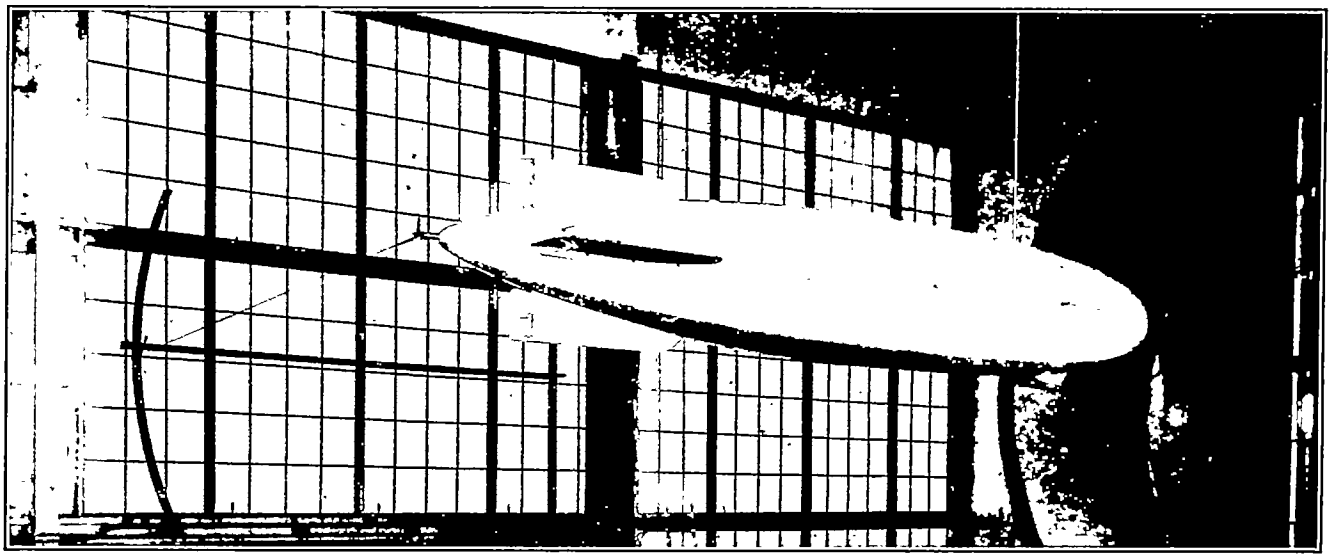

FIGURE 4.—The ¼o-scale model U. S. S. *Akron* mounted in the propeller-research wind tunnel. $\theta=0°$

The measurements of lift, drag, and pitching moment were made at three air speeds, approximately 70, 85, and 100 miles per hour, and at nine angles of pitch, $-3°$, $0°$, $3°$, $6°$, $9°$, $12°$, $15°$, $18°$, and $20°$. The elevator forces and hinge moments were measured at the above-mentioned speeds and pitch angles and at nine elevator angles, $0°$, $\pm 5°$, $\pm 10°$, $\pm 15°$, and $\pm 20°$. These latter measurements were repeated at the inter-

FIGURE 5.—The ¼o-scale model U. S. S. *Akron* mounted in the propeller-research wind tunnel. $\theta=20°$

mediate speed with the balancing vanes removed from the elevators. The drag of the bare hull was measured in two separate tests at speeds ranging from 28 to 100 miles per hour. In order to obtain the lower speeds (below 50 miles per hour) it was necessary to reduce the pitch of the wind-tunnel propeller. (Reference 5.) The drag of the model was also determined for a position several feet downstream from the first

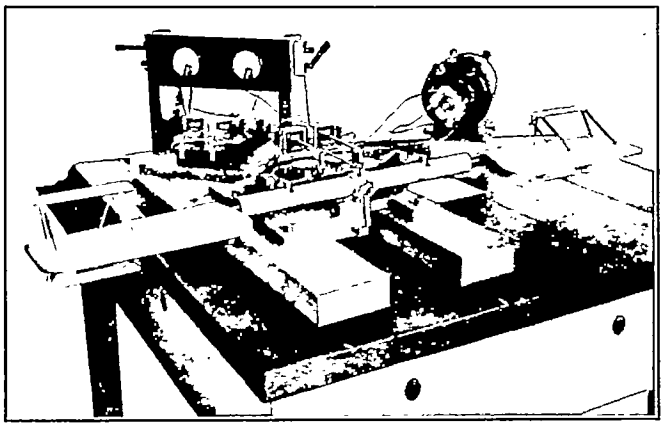

FIGURE 6.—Electric balance and auxiliary apparatus assembled for the calibration tests

at the high-speed range in order to obtain a check on the correction for the variation in static pressure along the axis of the tunnel.

The tare drag for four angles of pitch (0°, 6°, 12°, and 18°) was measured directly by suspending the model independently of the balances and supports and providing clearance for the horizontal steel crossbar and the tail sting. The latter was connected inside the hull to the crossbar, so that the total tare drag could be measured on the drag balance in the usual manner.

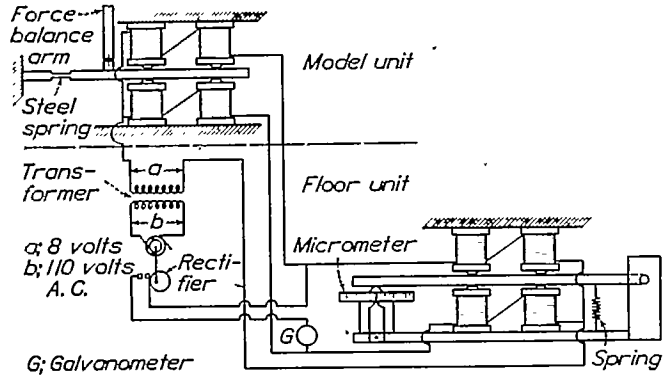

FIGURE 7.—Schematic drawing outlining principal features of the balance used in measuring the elevator forces and hinge moments

The range of Reynolds Numbers at which the tests were made varied from approximately 1,200,000 to 4,300,000. The maximum value was about one thirty-fourth that of the full-scale ship at a speed of 84 miles per hour. The Reynolds Number given above is $R_V = \frac{V(\text{vol})^{\frac{1}{3}}}{\nu} = 0.248\ R$, where R is the Reynolds Number based on the length of the hull.

PRECISION

In order to determine the deflection of the wire balance a reference mark on the model was observed before and during a drag test by means of a transit. The deflection, that is, the downstream movement of the model, observed at the maximum velocity of the tunnel with the hull at 0° pitch was approximately 0.06 inch. The error in the drag measurements caused by this deflection was 0.16 pound or less than 1 per cent of the gross drag of the bare hull.

The maximum deviation of the observed values of drag from a mean curve for the high-speed range was ±0.1 pound at the low angles of pitch and ±1 pound at the very high angles. The observed values of the lift were probably accurate to ±0.5 pound.

The electric balance in the calibration tests was accurate to ±0.02 pound; in the wind tunnel, however, because of the vibration of the model and the fluctuations in the air stream, the measurements of forces and moments on the elevators are probably only accurate to within ±0.1 pound for any individual force reading or ±0.1 inch-pound for any moment reading. The maximum elevator force and moment were approximately 20 pounds and 15 inch-pounds, respectively. A recalibration of the balance after the tests checked the previous calibration very satisfactorily for the uploads; that is, for loads corresponding to a down elevator. The download calibration, however, differed from the previous one by about 5 per cent. The reason for this discrepancy is not definitely known. Fortunately, the downloads are of less interest than the uploads which were measured more accurately.

RESULTS AND DISCUSSION

The results have been reduced to the usual nondimensional coefficients which are defined as follows:

$$\text{Drag coefficient, } C_S = \frac{\text{Drag}}{q\ (\text{vol})^{\frac{2}{3}}}$$

$$\text{Lift coefficient, } C_L = \frac{\text{Lift}}{q\ (\text{vol})^{\frac{2}{3}}}$$

$$\text{Moment coefficient, } C_m = \frac{\text{Moment about center of buoyancy}}{q\ \text{vol}}$$

$$\text{Elevator force coefficient, } C_E = \frac{\text{Elevator force normal to hull axis}}{q\ S}$$

$$\text{Elevator hinge moment coefficient } C_H = \frac{\text{Moments about elevator axis}}{q\ S\ c}$$

where q = dynamic pressure in pounds per square foot
vol = volume of hull in cubic feet,
S = area of elevators in square feet (not including balance vanes), and
c = chord of elevator in feet.

The faired coefficients are presented in Tables I, II, and III for the bare hull, the hull with the control car and Mark-I surfaces, and with the control car and Mark-II surfaces, respectively.

The drag coefficients are corrected for tare drag and for static pressure variation in the tunnel which amount

to about 38 per cent and 10 per cent, respectively, of the gross drag of the bare hull at 0° angle of pitch. The static pressure variation along the hull is given in the following table:

a/L	0	0.1	0.2	0.3	0.4	0.5	0.6	0.7	0.8	0.9	1.0
p/q	.032	.025	.020	.017	.015	.013	.011	.010	.010	.011	.013

density wind tunnel. A wooden model, one two-hundredths scale and of polygonal cross section similar to the model of the present tests, was tested both on the main balance and on the auxiliary balance in the old open-throat variable-density tunnel. (Reference 3.) A metal model, one two-hundred-fiftieth scale, had a circular cross section and was tested on the

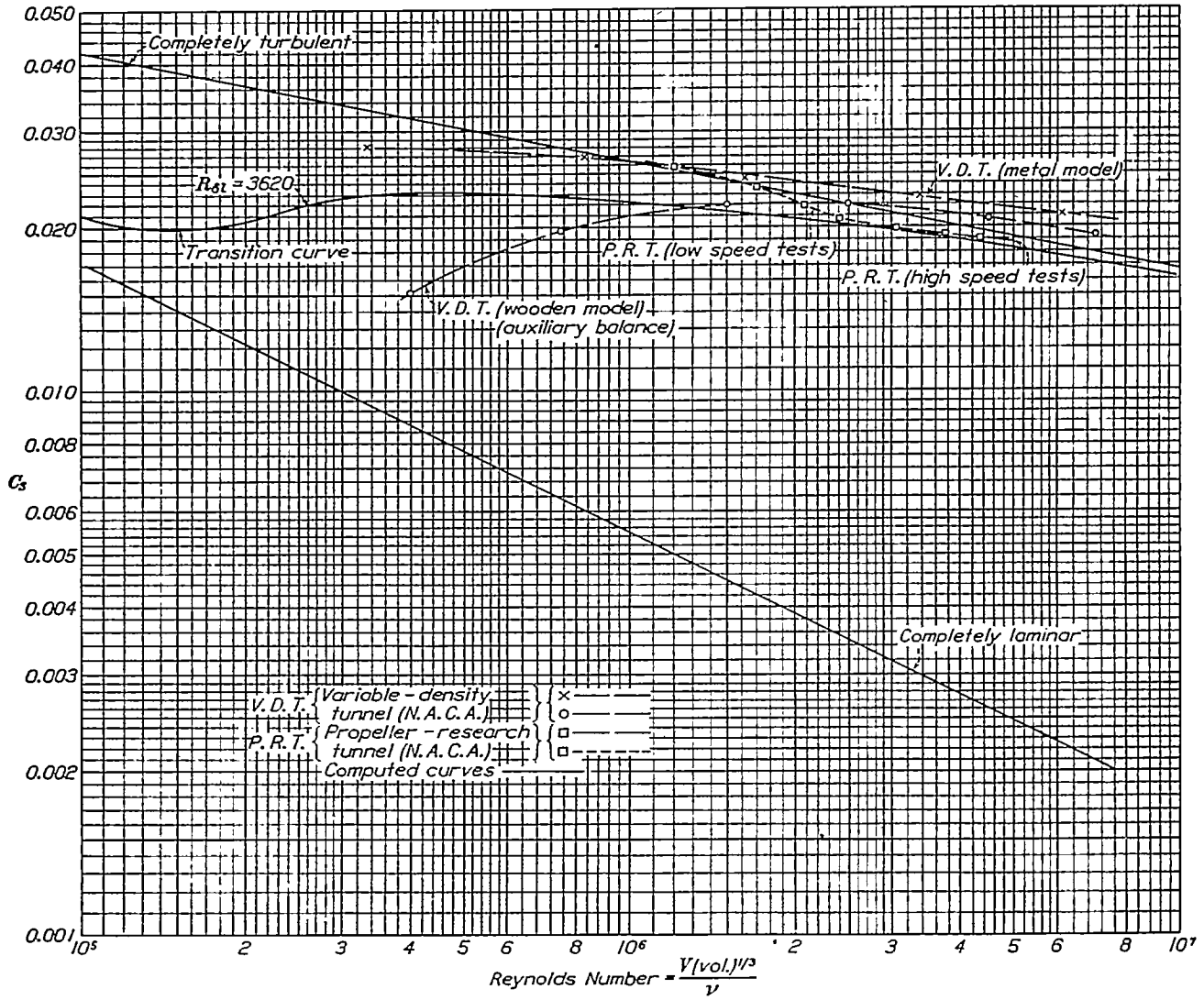

FIGURE 8.—Experimental drag coefficients and computed frictional-drag coefficients of bare hull for the 1/10-scale model U. S. S. *Akron*

where a is the distance from the nose, L the length of the hull, p the static pressure at a point on the axis of the tunnel, and q the dynamic pressure of the air stream.

The method of determining the latter correction was to plot the static pressure measured in the absence of the model at the points along the axis against the corresponding cross-sectional area of the hull and then to integrate the area under the resulting curve.

The drag coefficients of the bare hull for three values of the Reynolds Number are given in the following table and compared with the results obtained with two models of the same airship tested in the variable-

auxiliary balance in the new closed-throat arrangement of the variable-density tunnel. The results of the latter tests have not previously been published.

Reynolds Number $\left(\frac{V(\text{vol})^{\frac{1}{3}}}{\nu}\right)$		3,050,000	3,730,000	4,300,000
P. R. T. model ZRS-4 (one-fortieth scale)	C_S=	0.0193	0.0193	0.0190
V. D. T. wooden model (main balance) (one two-hundredth scale)	C_S=			.0180
V. D. T. wooden model (auxiliary balance) (one two-hundredth scale)	C_S=	.0215	.0212	.0209
V. D. T. metal model (auxiliary balance) (one two-hundred-fiftieth scale)	C_S=	.0223	.0223	.0219

The results of the present tests at the highest Reynolds Number are seen to be about a mean of the results obtained in the variable-density tunnel for the one two-hundredth scale wooden model. The agree-

ment is not quite so good, however, when the results are compared to those of the metal model, which are about 15 per cent higher than the present results. It should be noted, however, that the accuracy of the tests conducted in the old variable-density tunnel is somewhat questionable because of a very large horizontal buoyancy correction. Also, in the case of the tests on the main balance, the interference effects of the relatively large streamline supporting-strut are

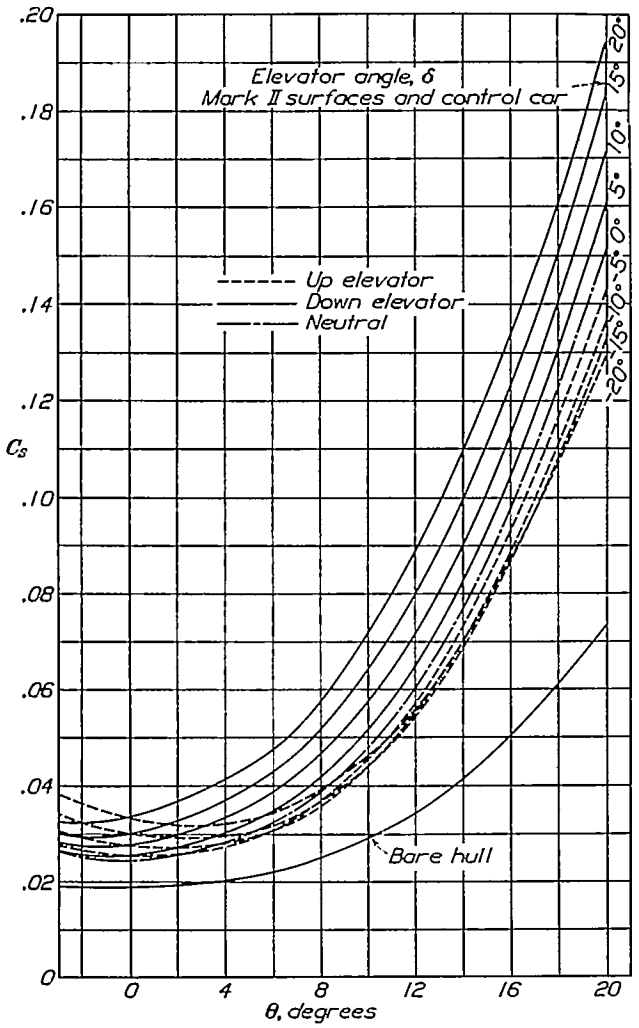

FIGURE 9.—Drag coefficients—bare hull and hull with Mark-II tail surfaces and control car (q=25.6 pounds per square foot) for the 1/40-scale model U. S. S. *Akron*

unknown. The difference between the present results and those of the new closed-throat variable-density tunnel, in which the buoyancy correction was quite small, might possibly be attributed to the difference in cross section between the two models. The drag coefficients are plotted against Reynolds Number in Figure 8 on logarithmic scales and compared with the variable-density tunnel results and also with the frictional drag for the present model computed by the method described in reference 6. The transition curve was computed for the critical boundary-layer Reynolds Number corresponding to the transition point found in the boundary-layer measurements. (Reference 2.)

The high-speed portion of the curve for the subject tests approximates that of the computed transition curve, whereas the low-speed values, contrary to what one would expect, increase with decreasing Reynolds Number until at the lowest speeds the curve approximates the computed curve for completely turbulent flow. This variation may possibly be accounted for

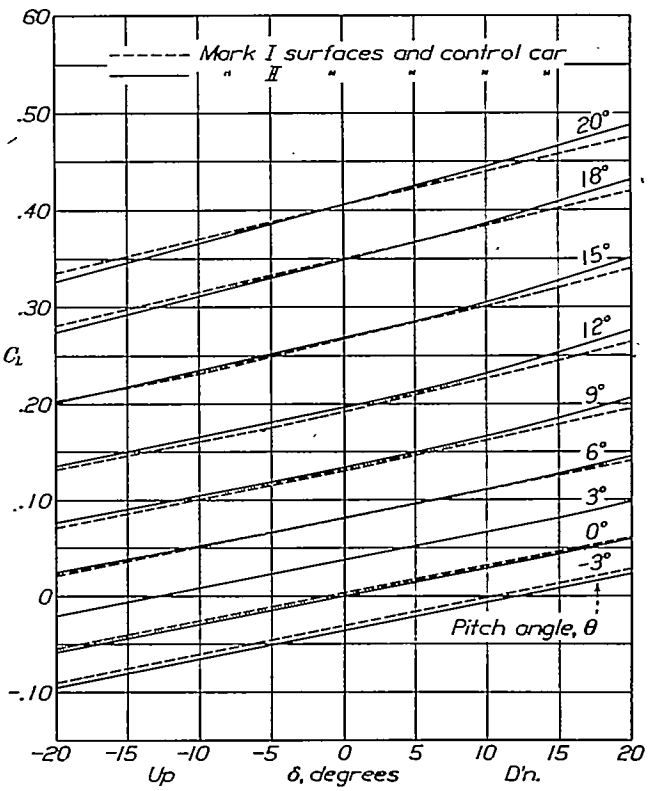

FIGURE 10.—Lift coefficients (q=25.6 pounds per square foot) for the 1/40-scale model U. S. S. *Akron*

by a change in the air-stream turbulence. If the degree of turbulence in the wind stream were the same for the low-speed as for the high-speed tests the experimental curve for the former would be expected to fall along the transition curve approximated by the high-speed drag values. The fact that the rate of increase of the drag coefficients, with decreasing Reynolds Number, is greater for the low-speed than for the high-speed test apparently indicates that the degree of turbulence in the air stream was greater for the low speeds, in which the pitch of the wind-tunnel propeller was decreased, than for the high speeds. The direct

comparison of the measured and frictional drag, as given above, is considered justified by the fact that the pressure drag on this model determined from pressure-distribution tests (reference 6) was negligible, within the accuracy of the tests.

The drag of the bare hull in the second position, about 7 feet downstream, was 12 per cent higher than for the first. These results are somewhat questionable, however, because of the unsteadiness of the model and the uncertainty of the tare drag in this position, both of which were due to the fact that the rear supporting wires were in the very turbulent backwash from the bell of the exit cone. If the tare drag determined for the first position is used in calculating the drag the difference is reduced to 8 per cent. The horizontal buoyancy correction for the second position

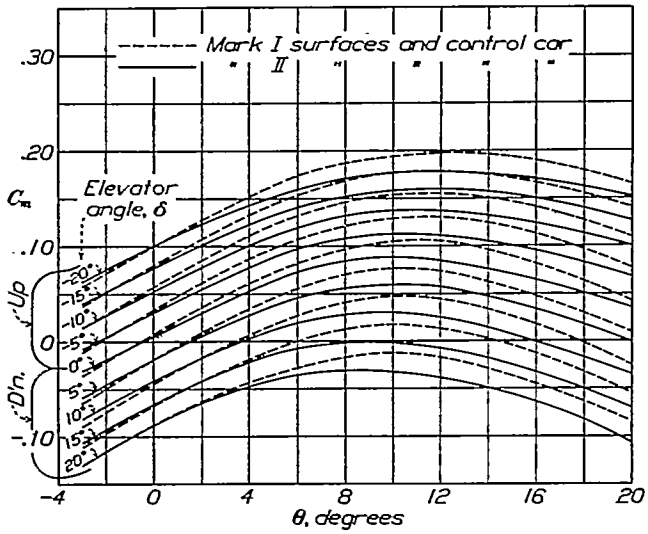

FIGURE 11.—Pitching-moment coefficients about center of buoyancy (q=25.6 pounds per square foot) for the 1/10-scale model U. S. S. *Akron*

was 6 per cent of the drag of the hull and was in the opposite direction to that of the upstream position.

The drag coefficients for the bare hull and for the hull fitted with the Mark-II surfaces and control car are shown in Figure 9 for the various angles of pitch. The Mark-II surfaces and control car increased the drag coefficient from 0.0190 to 0.0242, at 0° angle of pitch, an increase over the bare-hull drag of about 27 per cent. The results were approximately the same with the Mark-I surfaces at this angle of pitch. At other angles of pitch the Mark-I surfaces gave a somewhat lower drag coefficient than the Mark-II. A drag test of the hull with the control car showed that the contribution to the drag of this appendage was less than 3 per cent of the drag of the bare hull.

The lift coefficients for the hull with the tail surfaces, shown in Figure 10, are very little different for the two sets of tail surfaces although, in general, the Mark-II coefficients are slightly higher.

The pitching-moment coefficients, taken about the center of buoyancy, are given in Figure 11. The slopes of these curves indicate that the model, with either set of tail surfaces, is somewhat unstable for angles of pitch up to 9°, is then approximately neutrally stable for a small range, and is stable for pitch angles greater than 12°. The instability is somewhat less with Mark-II tail surfaces than with Mark-I.

The pitching-moment coefficients are considerably lower for the Mark-II fins and elevators than for the Mark-I, indicating that the former, although having approximately 10 per cent less area, should give better control. This indication is shown in a different manner in Figure 12, in which the elevator angles for zero moment, obtained from the intersection of the moment curves with the axis of abscissa (fig. 11), have been plotted for the corresponding angles of

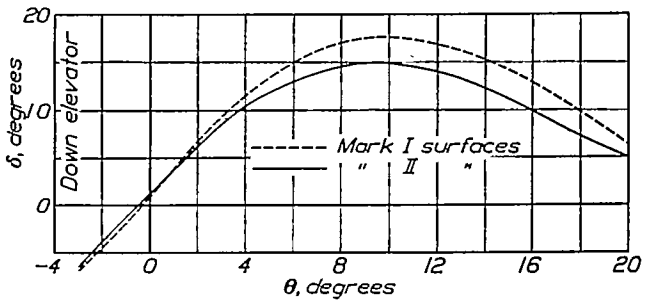

FIGURE 12.—Elevator angle required for zero moment. The 1/10-scale model U. S. S. *Akron*

pitch. From these curves may be determined the elevator angle required for zero pitching moment at any desired angle of pitch. The difference in the two curves is small at the low angles but increases with pitch angle to a maximum at about 10°, where the elevator angle required for zero moment with the Mark-II surfaces is nearly 3° less than with the Mark-I. The fact that the moment coefficients are not zero for the 0° angle of pitch at the 0° elevator setting indicates that there was a slight asymmetry in the model or that the air flow was not strictly axial.

The coefficients for the elevator forces normal to the axis of the hull are compared in Figure 13. The Mark-II coefficients are higher, in general, than the Mark-I, the difference being small at the low elevator angles but increasing with elevator angle to a maximum at 20°. The coefficients change very slowly with angle of pitch up to an angle of 10°. This slow change is probably because the direction of the local velocity over the elevators at the low pitch angles was controlled by, and was parallel to, the main fin

surfaces. As the angle of pitch increased the influence of the fixed fin surfaces decreased; hence, the elevator forces increased more rapidly.

The variation of the elevator hinge moments with elevator angle is shown in Figures 14 and 15 for five angles of pitch. The results for the two types of surfaces are similar in that they show that the elevators were considerably overbalanced for a very large range of elevator angles. In both cases the overbalance is

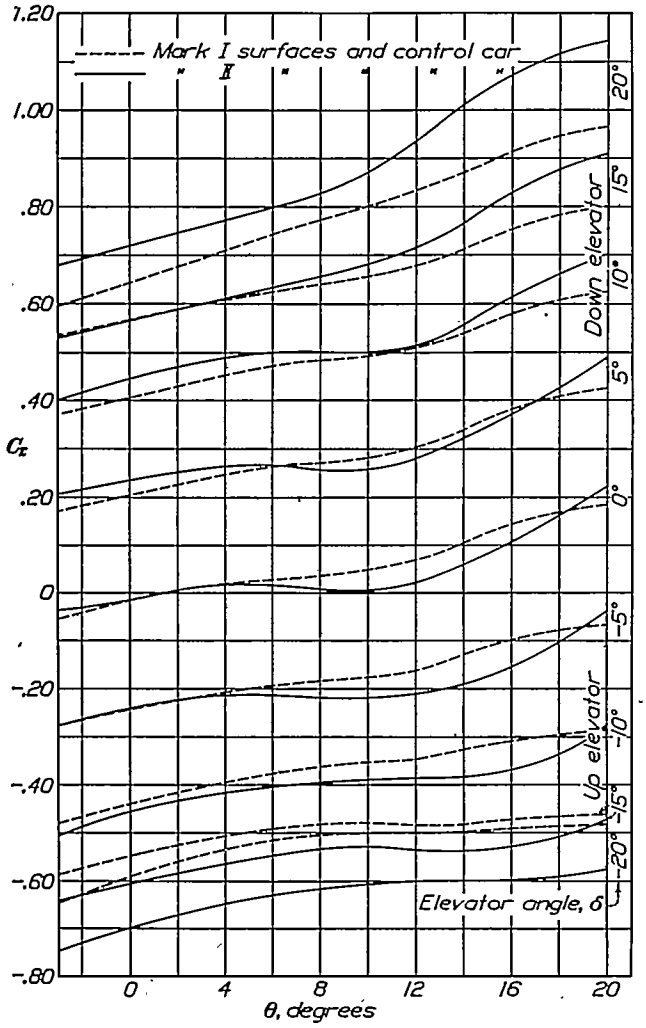

FIGURE 13.—Elevator force coefficients (q=25.6 pounds per square foot)

a maximum, for the low angles of pitch, at approximately $\delta = 8°$ and again at $\delta = -8°$. The overbalance with the Mark-I surfaces, however, is considerably less than with the Mark-II, as was to be expected, since the balancing vanes for the Mark-II surfaces were larger in proportion to the area of the elevator surface than those of the Mark-I, while the chord of the Mark-II elevators was about 10 per cent less than that of the Mark-I. A better method of comparing these surfaces is to compute the moments of the areas of the elevator surfaces and the balancing vanes about the elevator hinge axis, considering that the moments of the balancing vanes are opposed to those of the elevators. The moments for the Mark-II surfaces, if computed in this manner, are about 20 per cent less than those of the Mark-I.

149900—33——39

It is understood that in the design of the elevator surfaces a certain amount of overbalance was intended in order to overcome the friction in the control system

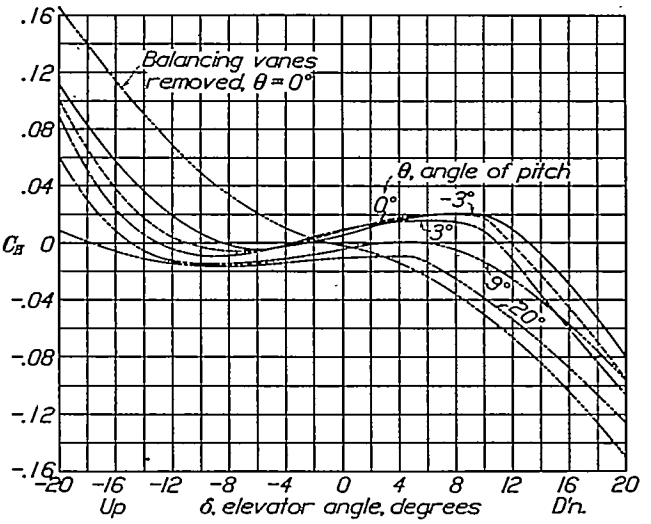

FIGURE 14.—Elevator hinge moment coefficients. The 1/40-scale model U. S. S. *Akron*. Mark-II tail surfaces. (q=25.6 pounds per square foot)

and, more particularly, to reduce the hinge moments at the high angles of these surfaces. The range and magnitude of the overbalance shown in the results of the present tests, however, seem to be excessive, especially in the case of the Mark-II control surfaces. The results of these tests have since been confirmed by full-scale flight tests.

The results of the elevator hinge moments and forces for the Mark-II elevators without the balancing vanes

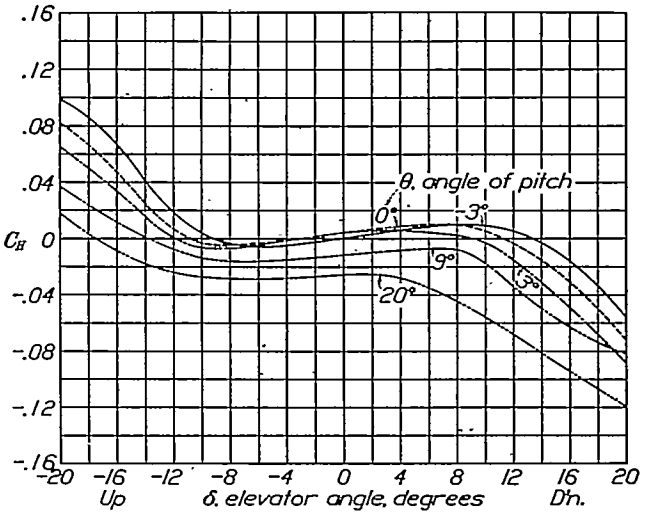

FIGURE 15.—Elevator hinge moment coefficients. The 1/40-scale model U. S. S. *Akron*. Mark-I tail surfaces. (q=25.6 pounds per square foot)

are presented in Table III–f and Table III–g, respectively. The hinge moments for the 0° angle of pitch are also included in the plot in Figure 13.

CONCLUSIONS

1. The drag of the bare hull at the high Reynolds Numbers was found to be in reasonable agreement with the results of previous tests on models of the same airship.

2. The Mark-II tail surfaces were found to give more favorable characteristics with respect to control than those of the Mark-I.

3. The results of the measurements of the elevator hinge moments showed that these coefficients were considerably greater for the Mark-II fins at the high elevator angles than for the Mark-I and that both sets of elevators were overbalanced for a large range of elevator angles, this overbalance appearing to be excessive for the Mark-II elevators.

LANGLEY MEMORIAL AERONAUTICAL LABORATORY,
NATIONAL ADVISORY COMMITTEE FOR AERONAUTICS,
LANGLEY FIELD, VA., *May 6, 1932.*

REFERENCES

1. Freeman, Hugh B.: Pressure-Distribution Measurements on the Hull and Fins of a 1/40-Scale Model of the U. S. Airship *Akron*. T. R. No. 443, N. A. C. A., 1932.
2. Freeman, Hugh B.: Measurements of Flow in the Boundary Layer of a 1/40-Scale Model of the U. S. Airship *Akron*. T. R. No. 430, N. A. C. A., 1932.
3. Abbott, Ira H.: Airship Model Tests in the Variable Density Wind Tunnel. T. R. No. 394, N. A. C. A., 1931.
4. Relf, E. F., and Simmons, L. F. G.: A Distant-Reading Instrument for the Measurement of Small Displacements. R. & M. 1092, British A. R. C., 1927.
5. Weick, Fred E., and Wood, Donald, H.: The Twenty-Foot Propeller Research Tunnel of the National Advisory Committee for Aeronautics. T. R. No. 300, N. A. C. A., 1928.
6. Millikan, Clark B.: The Boundary Layer and Skin Friction for a Figure of Revolution. Trans. A. S. M. E., vol. 54, No. 2, January 30, 1932.

TABLE I

1/40-SCALE MODEL U. S. S. "AKRON"

BARE HULL

LIFT, DRAG, AND PITCHING-MOMENT COEFFICIENTS

q	Angle of pitch, θ								
	−3°	0°	3°	6°	9°	12°	15°	18°	20°
	$C_D = \frac{D}{q\,(\text{vol})^{2/3}}$								
12.5	0.0199	0.0198	0.0208	0.0229	0.0280	0.0354	0.0478	0.0628	0.0873
19.0	.0193	.0193	.0202	.0222	.0273	.0346	.0467	.0619	.0751
25.6	.0191	.0190	.0200	.0219	.0270	.0342	.0460	.0613	.0737
	$C_L = \frac{L}{q\,(\text{vol})^{2/3}}$								
12.5	−0.006	0.000	0.011	0.029	0.054	0.080	0.115	0.155	0.183
19.0	−.006	.000	.011	.029	.054	.080	.115	.155	.183
25.6	−.006	.000	.011	.029	.054	.080	.115	.155	.183
	$C_m = \frac{M}{q\,\text{vol}}$								
12.5	−0.070	0.003	0.078	0.150	0.212	0.260	0.307	0.348	0.377
19.0	−.070	.003	.078	.150	.212	.260	.307	.348	.377
25.6	−.070	.003	.078	.150	.212	.260	.307	.348	.377

TABLE II–*a*

1/40-SCALE MODEL, U. S. S. "AKRON"

MARK I TAIL SURFACES

DRAG COEFFICIENTS

$$C_S = \frac{D}{q\,(\text{vol})^{2/3}}$$

δ	q	Angle of pitch, θ								
		−3°	0°	3°	6°	9°	12°	15°	18°	20°
−20°	12.5	0.0385	0.0331	0.0316	0.0343	0.0419	0.0580	0.0815	0.1117	0.1430
	19.0	.0380	.0327	.0310	.0336	.0411	.0563	.0780	.1090	.1385
	25.6	.0376	.0325	.0308	.0331	.0408	.0555	.0767	.1079	.1365
−15°	12.5	.0343	.0300	.0294	.0328	.0417	.0581	.0824	.1140	.1456
	19.0	.0338	.0296	.0288	.0323	.0408	.0566	.0797	.1116	.1412
	25.6	.0335	.0294	.0286	.0319	.0405	.0559	.0787	.1104	.1394
−10°	12.5	.0306	.0274	.0275	.0320	.0417	.0586	.0848	.1185	.1489
	19.0	.0301	.0269	.0270	.0314	.0406	.0573	.0820	.1160	.1450
	25.6	.0298	.0266	.0268	.0311	.0402	.0565	.0809	.1149	.1432
−5°	12.5	.0278	.0255	.0263	.0317	.0419	.0595	.0872	.1241	.1537
	19.0	.0272	.0250	.0259	.0311	.0410	.0583	.0846	.1211	.1496
	25.6	.0270	.0248	.0257	.0309	.0405	.0575	.0834	.1200	.1477
0°	12.5	.0263	.0246	.0260	.0323	.0435	.0615	.0907	.1306	.1604
	19.0	.0258	.0242	.0257	.0318	.0427	.0601	.0880	.1275	.1568
	25.6	.0256	.0240	.0255	.0314	.0421	.0591	.0868	.1261	.1544
5°	12.5	.0261	.0254	.0276	.0344	.0472	.0665	.0967	.1388	.1699
	19.0	.0257	.0249	.0273	.0339	.0465	.0651	.0941	.1354	.1655
	25.6	.0255	.0247	.0271	.0335	.0460	.0641	.0926	.1341	.1634
10°	12.5	.0269	.0272	.0306	.0380	.0520	.0732	.1019	.1483	.1806
	19.0	.0264	.0266	.0300	.0375	.0514	.0720	.1038	.1447	.1759
	25.6	.0262	.0265	.0298	.0371	.0509	.0714	.1007	.1436	.1742
15°	12.5	.0283	.0291	.0345	.0428	.0575	.0805	.1130	.1582	.1918
	19.0	.0279	.0292	.0339	.0420	.0569	.0795	.1111	.1548	.1867
	25.6	.0277	.0288	.0335	.0417	.0565	.0790	.1105	.1537	.1858
20°	12.5	.0314	.0334	.0390	.0489	.0635	.0882	.1232	.1686	.2035
	19.0	.0309	.0328	.0383	.0476	.0628	.0873	.1215	.1652	.1985
	25.6	.0306	.0325	.0378	.0468	.0625	.0868	.1211	.1644	.1977

TABLE II–*b*

LIFT COEFFICIENTS

$$C_L = \frac{L}{q\,(\text{vol})^{2/3}}$$

δ	q	Angle of pitch, θ								
		−3°	0°	3°	6°	9°	12°	15°	18°	20°
−20°	12.5	−0.090	−0.055	−0.020	0.021	0.075	0.139	0.210	0.290	0.344
	19.0	−.090	−.055	−.020	.021	.073	.136	.207	.285	.339
	25.6	−.090	−.055	−.020	.021	.071	.133	.204	.281	.335
−15°	12.5	−.075	−.040	−.006	.035	.089	.153	.225	.306	.361
	19.0	−.075	−.040	−.006	.035	.087	.149	.222	.302	.357
	25.6	−.075	−.040	−.006	.035	.085	.145	.219	.299	.353
−10°	12.5	−.061	−.026	.009	.049	.102	.167	.240	.321	.378
	19.0	−.061	−.026	.009	.049	.100	.163	.235	.317	.374
	25.6	−.061	−.026	.009	.049	.099	.160	.231	.314	.370
−5°	12.5	−.045	−.011	.023	.064	.119	.183	.257	.339	.396
	19.0	−.045	−.011	.023	.064	.116	.179	.252	.304	.391
	25.6	−.045	−.011	.023	.064	.114	.175	.247	.330	.386
0°	12.5	−.030	.004	.037	.079	.132	.199	.274	.356	.414
	19.0	−.030	.004	.037	.079	.130	.195	.270	.352	.409
	25.6	−.030	.004	.037	.079	.129	.191	.266	.348	.405
5°	12.5	−.017	.017	.052	.094	.150	.216	.290	.375	.431
	19.0	−.017	.017	.052	.094	.147	.213	.286	.370	.426
	25.6	−.017	.017	.053	.094	.145	.210	.282	.365	.421
10°	12.5	−.002	.031	.067	.110	.165	.232	.309	.392	.450
	19.0	−.002	.031	.067	.110	.163	.229	.305	.388	.445
	25.6	−.002	.031	.067	.110	.162	.226	.301	.385	.440
15°	12.5	.013	.046	.082	.125	.180	.250	.326	.410	.467
	19.0	.013	.046	.082	.125	.179	.247	.323	.405	.463
	25.6	.013	.046	.082	.125	.178	.245	.320	.401	.459
20°	12.5	.026	.060	.096	.140	.196	.267	.344	.427	.485
	19.0	.026	.060	.096	.140	.195	.264	.341	.423	.480
	25.0	.026	.060	.096	.140	.194	.262	.339	.420	.475

TABLE II–c

PITCHING-MOMENT COEFFICIENTS

$$C_m = \frac{M}{q\,\mathrm{vol}}$$

δ	q	Angle of pitch, θ								
		−3°	0°	3°	6°	9°	12°	15°	18°	20°
−20°	12.5	0.059	0.095	0.139	0.174	0.189	0.193	0.188	0.173	0.160
	19.0	.059	.095	.139	.174	.190	.195	.191	.176	.163
	25.6	.059	.095	.139	.174	.191	.196	.194	.179	.165
−15°	12.5	.039	.077	.120	.154	.170	.173	.165	.149	.135
	19.0	.039	.077	.120	.154	.172	.176	.168	.152	.138
	25.6	.039	.077	.120	.154	.173	.178	.170	.155	.140
−10°	12.5	.016	.055	.099	.131	.148	.150	.139	.120	.105
	19.0	.016	.055	.099	.131	.149	.153	.142	.123	.108
	25.6	.016	.055	.099	.131	.150	.155	.145	.125	.110
−5°	12.5	−.009	.025	.075	.107	.123	.125	.114	.091	.073
	19.0	−.009	.025	.075	.107	.124	.128	.116	.093	.075
	25.6	−.009	.025	.075	.107	.125	.130	.118	.095	.077
0°	12.5	−.036	.004	.050	.082	.098	.100	.084	.059	.039
	19.0	−.036	.004	.050	.082	.099	.103	.086	.061	.041
	25.6	−.036	.004	.050	.082	.100	.105	.088	.063	.043
5°	12.5	−.065	−.021	.022	.055	.069	.071	.051	.025	.003
	19.0	−.065	−.021	.022	.055	.072	.072	.053	.028	.006
	25.6	−.065	−.021	.022	.055	.074	.073	.055	.030	.009
10°	12.5	−.090	−.048	−.005	.027	.040	.039	.020	−.009	−.031
	19.0	−.090	−.048	−.005	.027	.043	.042	.023	−.005	−.028
	25.6	−.090	−.048	−.005	.027	.045	.044	.025	−.002	−.025
15°	12.5	−.111	−.069	−.030	.000	.013	.008	−.010	−.038	−.060
	19.0	−.111	−.069	−.030	.000	.014	.010	−.007	−.035	−.057
	25.6	−.111	−.069	−.030	.000	.015	.012	−.005	−.032	−.055
20°	12.5	−.130	−.087	−.054	−.029	−.017	−.021	−.040	−.068	−.088
	19.0	−.130	−.087	−.054	−.029	−.015	−.019	−.038	−.066	−.086
	25.6	−.130	−.087	−.054	−.029	−.014	−.017	−.037	−.064	−.084

TABLE II–d

ELEVATOR FORCE COEFFICIENTS

$$C_E = \frac{L_E}{qS}$$

δ	q	Angle of pitch, θ								
		−3°	0°	3°	6°	9°	12°	15°	18°	20°
−20°	12.5	−0.671	−0.615	−0.570	−0.536	−0.523	−0.523	−0.514	−0.502	−0.499
	19.0	−.659	−.604	−.559	−.525	−.511	−.511	−.504	−.492	−.488
	25.6	−.647	−.591	−.547	−.515	−.500	−.501	−.492	−.483	−.481
−15°	12.5	−.569	−.530	−.496	−.471	−.459	−.468	−.456	−.446	−.441
	19.0	−.580	−.541	−.508	−.482	−.470	−.477	−.467	−.456	−.451
	25.6	−.588	−.549	−.515	−.492	−.480	−.486	−.476	−.467	−.461
−10°	12.5	−.469	−.429	−.394	−.363	−.344	−.334	−.302	−.281	−.270
	19.0	−.475	−.435	−.400	−.370	−.351	−.342	−.310	−.288	−.278
	25.6	−.480	−.441	−.407	−.375	−.358	−.349	−.317	−.298	−.286
−5°	12.5	−.279	−.244	−.219	−.195	−.178	−.156	−.101	−.069	−.055
	19.0	−.279	−.244	−.219	−.195	−.178	−.158	−.105	−.074	−.060
	25.6	−.279	−.244	−.219	−.195	−.178	−.161	−.110	−.079	−.066
0°	12.5	−.053	−.019	.010	.028	.042	.073	.140	.174	.194
	19.0	−.053	−.019	.010	.028	.042	.071	.138	.170	190
	25.6	−.053	−.019	.010	.028	.042	.070	.135	.165	.185
5°	12.5	.165	.197	.231	.259	.273	.304	.364	.410	.425
	19.0	.168	.200	.234	.261	.273	.304	.364	.410	.425
	25.6	.171	.202	.236	.263	.273	.304	.364	.410	.425
10°	12.5	.356	.388	.425	.452	.470	.493	.544	.593	.610
	19.0	.363	.395	.433	.461	.479	.501	.551	.601	.617
	25.6	.371	.403	.440	.470	.487	.510	.559	.609	.624
15°	12.5	.496	.525	.566	.595	.621	.652	.709	.761	.781
	19.0	.515	.541	.580	.605	.635	.665	.721	.771	.791
	25.6	.534	.560	.598	.623	.648	.679	.733	.783	.800
20°	12.5	.577	.619	.676	.725	.771	.815	.873	.929	.949
	19.0	.586	.627	.685	.734	.779	.823	.885	.939	.957
	25.6	.595	.635	.693	.741	.788	.832	.896	.948	.965

TABLE II–e

HINGE MOMENT COEFFICIENT

$$C_H = \frac{M_H}{qSc}$$

δ	q	Angle of pitch, θ								
		−3°	0°	3°	6°	9°	12°	15°	18°	20°
−20°	12.5	0.097	0.079	0.062	0.046	0.033	0.024	0.019	0.015	0.013
	19.0	.098	.081	.064	.048	.035	.027	.022	.018	.016
	25.6	.099	.082	.065	.050	.037	.029	.025	.021	.018
−15°	12.5	.055	.036	.025	.015	.006	−.002	−.008	−.011	−.014
	19.0	.055	.036	.025	.015	.006	−.002	−.008	−.011	−.014
	25.6	.055	.036	.025	.015	.006	−.002	−.008	−.011	−.014
−10°	12.5	.007	−.001	−.004	−.006	−.011	−.017	−.018	−.021	−.025
	19.0	.005	−.003	−.006	−.008	−.013	−.018	−.019	−.022	−.026
	25.6	.004	−.004	−.007	−.009	−.014	−.019	−.020	−.023	−.027
−5°	12.5	−.006	−.003	−.003	−.008	−.015	−.020	−.018	−.023	−.027
	19.0	−.006	−.003	−.003	−.009	−.016	−.021	−.019	−.024	−.028
	25.6	−.006	−.003	−.003	−.009	−.016	−.022	−.020	−.025	−.029
0°	12.5	.000	.004	.004	−.002	−.011	−.016	−.014	−.020	−.024
	19.0	.000	.004	.004	−.002	−.012	−.017	−.015	−.021	−.025
	25.6	.000	.004	.004	−.002	−.012	−.018	−.016	−.022	−.026
5°	12.5	.007	.009	.005	.000	−.008	−.014	−.018	−.026	−.031
	19.0	.007	.009	.005	.000	−.008	−.014	−.018	−.026	−.031
	25.6	.007	.009	.005	.000	−.008	−.014	−.018	−.026	−.031
10°	12.5	.008	.002	−.005	−.013	−.022	−.030	−.040	−.054	−.062
	19.0	.009	.004	−.003	−.011	−.019	−.028	−.037	−.051	−.059
	25.6	.009	.005	−.002	−.009	−.017	−.025	−.034	−.048	−.056
15°	12.5	−.013	−.027	−.044	−.033	−.059	−.066	−.076	−.085	−.090
	19.0	−.011	−.025	−.042	−.031	−.058	−.065	−.076	−.084	−.089
	25.6	−.009	−.023	−.040	−.030	−.057	−.064	−.074	−.083	−.088
20°	12.5	−.055	−.072	−.088	−.084	−.082	−.089	−.100	−.113	−.120
	19.0	−.055	−.072	−.088	−.084	−.082	−.089	−.100	−.113	−.120
	25.6	−.055	−.072	−.088	−.084	−.082	−.089	−.100	−.113	−.120

TABLE III–a

1/40 SCALE MODEL U. S. S. "AKRON" MARK II TAIL SURFACES

DRAG COEFFICIENTS

$$C_S = \frac{D}{q(\text{vol})^{2/3}}$$

δ	q	Angle of pitch, θ								
		−3°	0°	3°	6°	9°	12°	15°	18°	20°
−20°	12.5	0.0395	0.0339	0.0325	0.0353	0.0446	0.0583	0.0808	0.1095	0.1345
	19.0	.0383	.0332	.0319	.0345	.0432	.0569	.0797	.1085	.1315
	25.6	.0383	.0335	0317	.0344	.0423	.0557	.0790	.1073	.1299
−15°	12.5	.0354	.0307	.0303	.0333	.0431	.0564	.0802	.1111	.1380
	19.0	.0344	.0301	.0297	.0320	.0412	.0556	.0790	.1093	.1357
	25.6	.0342	.0299	.0294	.0316	.0402	.0545	.0783	.1082	.1338
−10°	12.5	.0315	.0280	.0285	.0319	.0425	.0568	.0820	.1147	.1424
	19.0	.0310	.0275	.0280	.0311	.0410	.0663	.0806	.1127	.1401
	25.6	.0306	.0275	.0275	.0307	.0400	.0554	.0799	.1115	.1383
−5°	12.5	.0282	.0259	.0274	.0315	.0430	.0588	.0850	.1193	.1482
	19.0	.0281	.0255	.0268	.0311	.0418	.0570	.0839	.1178	.1455
	25.6	.0278	.0255	.0265	.0309	.0409	.0574	.0829	.1168	.1436
0°	12.5	.0259	.0247	.0269	.0324	.0447	.0618	.0893	.1258	.1560
	19.0	.0261	.0242	.0268	.0318	.0435	.0608	.0871	.1238	.1536
	25.6	.0262	.0242	.0268	.0320	.0430	.0605	.0872	.1231	.1514
5°	12.5	.0259	.0259	.0285	.0347	.0483	.0665	.0956	.1345	.1654
	19.0	.0265	.0256	.0285	.0343	.0470	.0656	.0941	.1321	.1632
	25.6	.0265	.0255	.0285	.0345	.0468	.0663	.0930	.1308	.1610
10°	12.5	.0276	.0281	.0320	.0390	.0535	.0733	.1045	.1443	.1762
	19.0	.0282	.0278	.0316	.0383	.0522	.0725	.1030	.1421	.1741
	25.6	.0280	.0275	.0314	.0383	.0521	.0720	.1017	.1407	.1717
15°	12.5	.0303	.0308	.0361	.0439	.0596	.0816	.1149	.1548	.1885
	19.0	.0300	.0305	.0354	.0432	.0583	.0808	.1133	.1530	.1855
	25.6	.0300	.0300	.0350	.0428	.0583	.0801	.1118	.1512	.1833
20°	12.5	.0335	.0338	.0407	.0495	.0663	.0909	.1264	.1655	.2018
	19.0	.0324	.0334	.0396	.0487	.0651	.0897	.1242	.1643	.1970
	25.6	.0324	.0336	.0389	.0477	.0650	.0890	.1227	.1621	.1950

TABLE III–b

LIFT COEFFICIENTS

$$C_L = \frac{L}{q(\text{vol})^{2/3}}$$

δ	q	Angle of pitch, θ								
		−3°	0°	3°	6°	9°	12°	15°	18°	20°
−20°	12.5	−0.095	−0.059	−0.020	0.025	0.080	0.143	0.211	0.284	0.334
	19.0	−.096	−.060	−.021	.024	.077	.137	.205	.279	.330
	25.6	−.095	−.059	−.021	.024	.077	.135	.201	.273	.326
−15°	12.5	−.080	−.045	−.006	.039	.095	.157	.225	.300	.351
	19.0	−.081	−.045	−.006	.039	.092	.153	.222	.297	.349
	25.6	−.080	−.045	−.006	.038	.091	.150	.218	.292	.347
−10°	12.5	−.065	−.029	.009	.054	.107	.171	.241	.317	.372
	19.0	−.065	−.030	.008	.053	.105	.167	.237	.313	.368
	25.6	−.065	−.030	.008	.051	.105	.165	.234	.311	.366
−5°	12.5	−.051	−.015	.024	.070	.122	.186	.257	.335	.391
	19.0	−.050	−.015	.023	.067	.119	.182	.253	.331	.388
	25.6	−.050	−.015	.023	.066	.119	.180	.250	.329	.386
0°	12.5	−.035	.000	.039	.084	.138	.203	.275	.355	.410
	19.0	−.036	.000	.038	.081	.135	.199	.271	.351	.407
	25.6	−.035	.000	.037	.081	.133	.196	.267	.349	.406
5°	12.5	−.021	.015	.053	.100	.156	.222	.294	.374	.430
	19.0	−.021	.015	.053	.097	.152	.216	.289	.370	.428
	25.6	−.020	.015	.052	.095	.149	.212	.284	.366	.425
10°	12.5	−.006	.029	.069	.115	.174	.240	.312	.392	.447
	19.0	−.006	.029	.067	.113	.170	.235	.308	.390	.447
	25.6	−.006	.029	.067	.111	.166	.232	.305	.388	.446
15°	12.5	.009	.045	.084	.132	.191	.258	.332	.413	.471
	19.0	.008	.044	.084	.130	.188	.253	.328	.412	.470
	25.6	.008	.044	.082	.128	.185	.253	.327	.409	.466
20°	12.5	.024	.061	.101	.151	.210	.279	.353	.433	.491
	19.0	.024	.061	.101	.149	.208	.277	.351	.432	.490
	25.6	.025	.058	.098	.143	.206	.276	.351	.431	.488

TABLE III–c

PITCHING-MOMENT COEFFICIENT

$$C_m = \frac{M}{q\,\text{vol}}$$

δ	q	Angle of pitch, θ								
		−3°	0°	3°	6°	9°	12°	15°	18°	20°
−20°	12.5	0.056	0.096	0.133	0.161	0.172	0.176	0.173	0.160	0.150
	19.0	.057	.093	.128	.158	.173	.176	.173	.162	.151
	25.6	.063	.101	.133	.159	.174	.178	.173	.163	.151
−15°	12.5	.037	.076	.113	.142	.155	.157	.150	.137	.126
	19.0	.039	.077	.113	.142	.156	.162	.157	.142	.127
	25.6	.040	.077	.112	.142	.156	.159	.154	.140	.127
−10°	12.5	.017	.054	.091	.124	.135	.136	.127	.110	.096
	19.0	.019	.056	.090	.117	.135	.140	.131	.113	.097
	25.6	.015	.053	.089	.120	.135	.137	.129	.113	.099
−5°	12.5	−.008	.032	.069	.100	.113	.112	.101	.081	.065
	19.0	−.006	.032	.067	.098	.112	.112	.101	.081	.065
	25.6	−.007	.031	.067	.097	.112	.111	.100	.082	.063
0°	12.5	−.034	.007	.046	.078	.090	.085	.070	.048	.030
	19.0	−.032	.007	.045	.075	.087	.085	.070	.048	.030
	25.6	−.032	.006	.043	.073	.087	.084	.070	.050	.035
5°	12.5	−.063	−.020	.021	.050	.061	.057	.040	.014	−.007
	19.0	−.059	−.017	.020	.048	.060	.057	.038	.013	−.006
	25.6	−.058	−.019	.018	.047	.058	.057	.040	.017	.000
10°	12.5	−.087	−.042	−.004	.022	.030	.026	.005	−.022	−.043
	19.0	−.084	−.042	−.005	.020	.030	.026	.007	−.020	−.041
	25.6	−.081	−.042	−.005	.021	.030	.025	.007	−.016	−.035
15°	12.5	−.109	−.065	−.028	−.007	−.003	−.010	−.030	−.058	−.078
	19.0	−.106	−.064	−.030	−.007	−.002	−.008	−.027	−.055	−.075
	25.6	−.107	−.065	−.029	−.007	−.002	−.007	−.024	−.050	−.071
20°	12.5	−.128	−.086	−.054	−.035	−.035	−.042	−.066	−.093	−.112
	19.0	−.125	−.085	−.055	−.036	−.032	−.043	−.061	−.087	−.107
	25.6	−.130	−.088	−.055	−.035	−.031	−.039	−.056	−.084	−.106

TABLE III–*d*

ELEVATOR FORCE COEFFICIENT

$$C_E = \frac{L_E}{qS}$$

δ	q	Angle of pitch, θ								
		−3°	0°	3°	6°	9°	12°	15°	18°	20°
−20°	12.5	−0.748	−0.700	−0.667	−0.647	−0.610	−0.600	−0.590	−0.577	−0.555
	19.0	−.748	−.700	−.666	−.645	−.610	−.600	−.594	−.582	−.558
	25.6	−.748	−.699	−.660	−.632	−.610	−.600	−.600	−.591	−.575
−15°	12.5	−.620	−.570	−.540	−.521	−.495	−.494	−.513	−.487	−.445
	19.0	−.630	−.578	−.559	−.535	−.507	−.512	−.523	−.495	−.456
	25.6	−.641	−.604	−.575	−.548	−.530	−.534	−.535	−.508	−.470
−10°	12.5	−.493	−.446	−.418	−.400	−.393	−.383	−.365	−.315	−.244
	19.0	−.497	−.450	−.422	−.405	−.393	−.385	−.370	−.326	−.260
	25.6	−.505	−.457	−.425	−.405	−.394	−.386	−.380	−.337	−.271
−5°	12.5	−.270	−.232	−.215	−.215	−.219	−.204	−.165	−.088	−.022
	19.0	−.273	−.234	−.216	−.215	−.220	−.209	−.170	−.095	−.029
	25.6	−.277	−.240	−.217	−.215	−.220	−.210	−.175	−.100	−.037
0°	12.5	−.045	−.020	.010	.014	.005	.027	.089	.180	.255
	19.0	−.038	−.016	.011	.014	.005	.023	.086	.171	.241
	25.6	−.034	−.015	.012	.015	.005	.021	.084	.163	.222
5°	12.5	.191	.230	.253	.259	.249	.280	.347	.426	.491
	19.0	.193	.235	.255	.262	.251	.280	.347	.426	.491
	25 6	.205	.237	.259	.264	.253	.280	.347	.426	.491
10°	12.5	.383	.423	.451	.464	.466	.483	.570	.645	.685
	19.0	.394	.434	.465	.483	.486	.496	.579	.662	.696
	25.6	.403	.446	.480	.500	.499	.511	.588	.662	.703
15°	12.5	.509	.540	.572	.606	.645	.701	.783	.860	.891
	19.0	.519	.550	.583	.620	.659	.708	.791	.867	.900
	25.6	.530	.564	.600	.635	.668	.712	.800	.876	.909
20°	12.5	.645	.696	.741	.780	.828	.898	.995	1.056	1.078
	19.0	.658	.707	.752	.791	.840	.912	1.022	1.088	1.110
	25.6	.681	.720	.760	.800	.849	.933	1.047	1.115	1.141

TABLE III–*e*

HINGE MOMENT COEFFICIENT

$$C_H = \frac{M_H}{qSc}$$

δ	q	Angle of pitch, θ								
		−3°	0°	3°	6°	9°	12°	15°	18°	20°
−20°	12.5	0.113	0.099	0.089	0.072	0.059	0.044	0.031	0.018	0.008
	19.0	.113	.099	.089	.072	.059	.045	.031	.017	.009
	25.6	.112	.100	.089	.072	.059	.045	.031	.017	.009
−15°	12.5	.048	.024	.016	.008	.002	−.004	−.005	−.009	−.009
	19.0	.047	.025	.014	.007	.001	−.003	−.006	−.008	−.009
	25.6	.046	.026	.013	.005	.000	−.003	−.006	−.008	−.009
−10°	12.5	.006	−.003	−.009	−.011	−.013	−.014	−.015	−.015	−.014
	19.0	.006	−.003	−.009	−.013	−.015	−.015	−.016	−.016	−.015
	25.6	.006	−.003	−.009	−.014	−.015	−.017	−.017	−.017	−.016
−5°	12.5	−.007	−.004	−.003	−.006	−.011	−.016	−.018	−.017	−.013
	19.0	−.005	−.004	−.004	−.007	−.012	−.018	−.019	−.018	−.014
	25.6	−.004	−.004	−.005	−.009	−.013	−.019	−.021	−.019	−.015
0°	12.5	.006	.010	.011	.007	−.003	−.012	−.015	−.013	−.009
	19.0	.005	.009	.010	.006	−.003	−.013	−.016	−.014	−.010
	25.6	.005	.008	.009	.006	−.005	−.014	−.018	−.015	−.011
5°	12.5	.018	.019	.023	.012	.003	−.005	−.008	−.010	−.013
	19.0	.018	.019	.023	.011	.001	−.005	−.009	−.011	−.012
	25.6	.018	.019	.016	.009	.001	−.007	−.010	−.011	−.010
10°	12.5	.018	.016	.009	−.001	−.015	−.022	−.031	−.039	−.046
	19.0	.019	.017	.009	−.001	−.014	−.023	−.030	−.037	−.044
	25.6	.020	.018	.009	−.001	−.013	−.024	−.029	−.036	−.040
15°	12.5	−.019	−.034	−.049	−.060	−.050	−.054	−.063	−.074	−.085
	19.0	−.018	−.034	−.049	−.050	−.050	−.054	−.061	−.071	−.084
	25.6	−.018	−.034	−.049	−.050	−.049	−.053	−.060	−.070	−.078
20°	12.5	−.081	−.097	−.107	−.099	−.096	−.096	−.102	−.112	−.126
	19.0	−.080	−.096	−.107	−.099	−.096	−.096	−.102	−.112	−.126
	25.6	−.079	−.095	−.106	−.099	−.096	−.096	−.102	−.112	−.126

TABLE III–*f*

BALANCING VANES REMOVED

HINGE MOMENT COEFFICIENT

$$C_H=\frac{M_H}{qSc}$$

δ	q	Angle of pitch, θ								
		−3°	0°	3°	6°	9°	12°	15°	18°	20°
−20°	19	0.189	0.165	0.147	0.135	0.128	0.130	0.129	0.119	0.113
−15°	19	.123	.104	.090	.080	.074	.073	.074	.075	.076
−10°	19	.066	.050	.040	.035	.035	.040	.046	.046	.039
−5°	19	.025	.015	.011	.012	.017	.019	.015	.006	−.003
0°	19	.001	−.002	−.004	−.005	−.006	−.009	−.017	−.029	−.039
5°	19	−.018	−.020	−.028	−.034	−.039	−.047	−.059	−.074	−.086
10°	19	−.044	−.052	−.067	−.075	−.082	−.093	−.108	−.125	−.137
15°	19	−.082	−.095	−.113	−.124	−.131	−.143	−.159	−.177	−.190
20°	19	−.136	−.151	−.172	−.180	−.186	−.200	−.217	−.235	−.248

TABLE III–*g*

ELEVATOR FORCE COEFFICIENT

$$C_E=\frac{L_H}{qS}$$

δ	q	Angle of pitch, θ								
		−3°	0°	3°	6°	9°	12°	15°	18°	20°
−20°	19	−0.610	−0.528	−0.475	−0.442	−0.421	−0.409	−0.400	−0.398	−0.390
−15°	19	−.429	−.370	−.332	−.309	−.294	−.284	−.285	−.290	−.292
−10°	19	−.280	−.234	−.209	−.197	−.190	−.191	−.196	−.183	−.160
−5°	19	−.155	−.125	−.109	−.100	−.095	−.079	−.057	−.028	−.001
0°	19	−.009	.007	.017	.023	.034	.060	.094	.133	.104
5°	19	.116	.127	.157	.170	.188	.220	.259	.303	.334
10°	19	.247	.267	.312	.340	.360	.391	.433	.480	.517
15°	19	.373	.400	.462	.498	.521	.563	.615	.662	.671
20°	19	.519	.560	.633	.682	.705	.750	.800	.838	.863